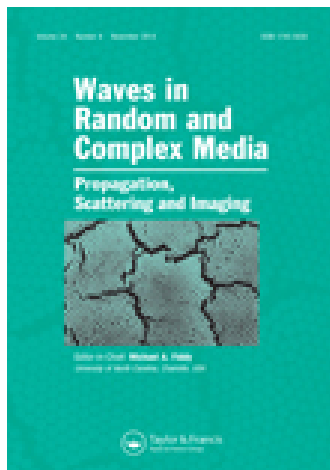


This article was downloaded by: [US Naval Academy]

On: 04 June 2015, At: 09:05

Publisher: Taylor & Francis

Informa Ltd Registered in England and Wales Registered Number: 1072954 Registered office: Mortimer House, 37-41 Mortimer Street, London W1T 3JH, UK



Waves in Random and Complex Media

Publication details, including instructions for authors and subscription information:

<http://www.tandfonline.com/loi/twrm20>

Polarization-induced reduction in scintillation of optical beams propagating in simulated turbulent atmospheric channels

S. Avramov-Zamurovic^a, C. Nelson^c, R. Malek-Madani^b & O. Korotkova^d

^a Department of Weapons and Systems Engineering, US Naval Academy, Annapolis, MD, USA

^b Department of Mathematics, US Naval Academy, Annapolis, MD, USA

^c Department of Electrical and Computer Engineering, US Naval Academy, Annapolis, MD, USA

^d Department of Physics, University of Miami, Coral Gables, FL, USA

Published online: 06 Nov 2014.



CrossMark

[Click for updates](#)

To cite this article: S. Avramov-Zamurovic, C. Nelson, R. Malek-Madani & O. Korotkova (2014) Polarization-induced reduction in scintillation of optical beams propagating in simulated turbulent atmospheric channels, *Waves in Random and Complex Media*, 24:4, 452-462, DOI: [10.1080/17455030.2014.944242](https://doi.org/10.1080/17455030.2014.944242)

To link to this article: <http://dx.doi.org/10.1080/17455030.2014.944242>

PLEASE SCROLL DOWN FOR ARTICLE

Taylor & Francis makes every effort to ensure the accuracy of all the information (the "Content") contained in the publications on our platform. However, Taylor & Francis, our agents, and our licensors make no representations or warranties whatsoever as to the accuracy, completeness, or suitability for any purpose of the Content. Any opinions and views expressed in this publication are the opinions and views of the authors, and are not the views of or endorsed by Taylor & Francis. The accuracy of the Content should not be relied upon and should be independently verified with primary sources of information. Taylor and Francis shall not be liable for any losses, actions, claims, proceedings, demands, costs, expenses, damages, and other liabilities whatsoever or howsoever caused arising directly or indirectly in connection with, in relation to or arising out of the use of the Content.

This article may be used for research, teaching, and private study purposes. Any substantial or systematic reproduction, redistribution, reselling, loan, sub-licensing, systematic supply, or distribution in any form to anyone is expressly forbidden. Terms & Conditions of access and use can be found at <http://www.tandfonline.com/page/terms-and-conditions>

Polarization-induced reduction in scintillation of optical beams propagating in simulated turbulent atmospheric channels

S. Avramov-Zamurovic^{a*}, C. Nelson^c, R. Malek-Madani^b and O. Korotkova^d

^aDepartment of Weapons and Systems Engineering, US Naval Academy, Annapolis, MD, USA;

^bDepartment of Mathematics, US Naval Academy, Annapolis, MD, USA; ^cDepartment of Electrical and Computer Engineering, US Naval Academy, Annapolis, MD, USA; ^dDepartment of Physics, University of Miami, Coral Gables, FL, USA

(Received 24 February 2014; accepted 9 July 2014)

It is experimentally demonstrated that the class of partially coherent, partially polarized optical beams can be efficiently used for reduction in scintillations on propagation through turbulent air. The experiment involving the electromagnetic beam generation and its interaction with turbulent air simulator is discussed in details. The collected data is in solid agreement with the recently published theoretical predictions.

1. Introduction

The atmospheric turbulence affecting optical beams can be efficiently mitigated via various techniques: source partial coherence,[1–5] aperture averaging,[6] sparse aperture detectors,[7,8] wavelength diversity,[9] and source temporal variations.[10] Recently, it was also proposed via analytical calculations [11] and simulations [12,13] that the polarization diversity can be efficient for solving this problem. In particular, in [12], a beam generated by a deterministic electromagnetic source being a combination of two Laguerre modes was shown to lead to considerable scintillation reduction with certain choice of mode parameters. In [11,13], partially coherent electromagnetic beams of Gaussian Schell-model class were shown to cut the scintillation in half, provided the orthogonal electric field components are uncorrelated.

The aim of this paper is to prove the results of [11,13] experimentally, demonstrating that a random electromagnetic beam with partial polarization propagating in a turbulent air channel has lower scintillation level compared to its scalar counterpart. One crucial step taken for achieving this goal is generation of this class of beams in a fully controllable manner. Although several techniques exist for generation of random electromagnetic beams,[14–17] we develop a novel optical setup which uses the interferometric approach together with two reflective spatial light modulators (SLM) providing readily adjustable phase modulation of both polarization components. High spatial resolution and tunable rate of cycling of the SLMs with full computer control allow for beam design with practically unlimited phase spatiotemporal correlation control in both polarization directions. The limiting case of two stationary frames on the SLMs (with

*Corresponding author. Email: avramov@usna.edu

the same or different realizations) is also of interest and is explored in detail. The phase screens for the SLMs can be prepared with the help of a recently developed method [18] and they obey single-point Gaussian statistics with desirable two-point correlation function. For this paper, correlation functions leading to Multi-Gaussian Schell-model beams [19–21] have been used because of their flat far-field intensity profiles convenient for uniform field detection. The turbulence simulator is designed as a chamber with hot air flowing in two orthogonal directions and allows for potential (see also [22]) and anisotropic conditions.

To our knowledge there exists only one report [23], which explores a similar effect. However, it is devoted to comparison of radially polarized vs. linearly polarized beams for scintillation reduction, uses a different method for beam generation, based on a single rotating diffuser, and does not relate the results to the beam polarization properties.

2. Theoretical background

The second-order correlation properties of a wide-sense statistically stationary electromagnetic beam can be described by means of the beam coherence–polarization matrix [24] or cross-spectral density matrix [25] whose spatial counterparts have the same form:

$$\overleftrightarrow{J}(\mathbf{r}_1, \mathbf{r}_2) = \begin{pmatrix} \langle E_x^*(\mathbf{r}_1)E_x(\mathbf{r}_2) \rangle & \langle E_x^*(\mathbf{r}_1)E_y(\mathbf{r}_2) \rangle \\ \langle E_y^*(\mathbf{r}_1)E_x(\mathbf{r}_2) \rangle & \langle E_y^*(\mathbf{r}_1)E_y(\mathbf{r}_2) \rangle \end{pmatrix}. \quad (1)$$

Here, \mathbf{r}_1 and \mathbf{r}_2 are the position vectors of two points in space, E_x and E_y are two mutually orthogonal components of the electric field vector transverse to direction of beam propagation, * denotes complex conjugate, and angular brackets represent either long-time or ensemble average.

If the instantaneous intensity of the beam is denoted by $i(\mathbf{r})$, then the average intensity of the beam is deduced from matrix (1) by the formula

$$i^{(I)}(\mathbf{r}) = \langle i(\mathbf{r}) \rangle = \text{Tr} \overleftrightarrow{J}(\mathbf{r}, \mathbf{r}) \quad (2)$$

Further, the conventional measure of the intensity fluctuations' contrast at a single position in an optical wave is its normalized variance or the *scintillation index*, defined as

$$c(\mathbf{r}) = \frac{i^{(II)}(\mathbf{r}) - [i^{(I)}(\mathbf{r})]^2}{[i^{(I)}(\mathbf{r})]^2}, \quad (3)$$

where $i^{(II)}(\mathbf{r}) = \langle i(\mathbf{r})^2 \rangle$ is the second moment of the instantaneous intensity $i(\mathbf{r})$. As is shown in [11], the scintillation index of an electromagnetic beam may be expressed in an alternative form:

$$c(\mathbf{r}) = \frac{c_{xx}(\mathbf{r})[i_x^{(I)}(\mathbf{r})]^2 + 2c_{xy}(\mathbf{r})i_x^{(I)}(\mathbf{r})i_y^{(I)}(\mathbf{r}) + c_{yy}(\mathbf{r})[i_y^{(I)}(\mathbf{r})]^2}{[i_x^{(I)}(\mathbf{r}) + i_y^{(I)}(\mathbf{r})]^2}. \quad (4)$$

In this representation, $i_x^{(I)}$ and $i_y^{(I)}$ are the intensities of x and y components of the electric field, i.e.

$$i_x^{(I)}(\mathbf{r}) = J_{xx}(\mathbf{r}), \quad i_y^{(I)}(\mathbf{r}) = J_{yy}(\mathbf{r}), \quad (5)$$

while $c_{xx}(\mathbf{r})$, $c_{yy}(\mathbf{r})$ are the scintillation indexes of the intensities fluctuating in two orthogonal directions and $c_{xy}(\mathbf{r})$ is that for their mutual intensity:

$$c_{\alpha\beta}(\mathbf{r}) = \frac{\langle i_\alpha(\mathbf{r})i_\beta(\mathbf{r}) \rangle - i_\alpha^{(I)}(\mathbf{r})i_\beta^{(I)}(\mathbf{r})}{i_\alpha^{(I)}(\mathbf{r})i_\beta^{(I)}(\mathbf{r})}, \quad (\alpha, \beta = x, y) \quad (6)$$

An important result relating to fields with uncorrelated field components [zero off-diagonal correlations of matrix (1)] immediately follows from formula (4): $c_{xy}(\mathbf{r})$ vanish leading to a reduction in the scintillation index compared to that for fully or partially correlated field components [non-zero off-diagonal correlations of matrix (1)]. In the limiting case of an unpolarized light beam, i.e. that with uncorrelated electric field components with equal intensities $i_x = i_y$, the scintillation index can be readily shown to be reduced by a factor of two, compared to an equivalent polarized beam.[11]

It will be convenient for detection of intensity statistics and polarization properties to generate electromagnetic beams with flat intensity profiles. A recently developed model for such a beam [21] gives for the elements of matrix (1) in the source plane the expressions:

$$J_{\alpha\beta}^{(0)}(\boldsymbol{\rho}_{10}, \boldsymbol{\rho}_{20}) = \frac{\sqrt{I_\alpha^0} \sqrt{I_\beta^0} B_{\alpha\beta}}{C_0} \exp\left(-\frac{\boldsymbol{\rho}_{10}^2 + \boldsymbol{\rho}_{20}^2}{4\sigma^2}\right) \sum_{m=1}^M \frac{(-1)^{m-1}}{m} \binom{M}{m} \exp\left[-\frac{|\boldsymbol{\rho}_{20} - \boldsymbol{\rho}_{10}|^2}{2m\delta_{\alpha\beta}^2}\right],$$

$$C_0 = \sum_{m=1}^M \frac{(-1)^{m-1}}{m} \binom{M}{m}. \quad (7)$$

Here, $\boldsymbol{\rho}_{10}$ and $\boldsymbol{\rho}_{20}$ are two-dimensional position vectors of two points in the source plane, I_α^0 ($\alpha = x, y$) are initial intensities in x and y directions, σ is the r.m.s. width of the beam, $\delta_{\alpha\beta}$, and $B_{\alpha\beta}$ are the r.m.s. width of the correlation and the single-point correlation coefficient between two electric field components, respectively. Also the properties of correlation matrix (1) require that $B_{xx} = B_{yy} = 1$, $|B_{xy}| = |B_{yx}|$, $\delta_{xy} = \delta_{yx}$. [21] In our experimental demonstration, we will only be concerned with uncorrelated field components, E_x and E_y , when $B_{xy} = B_{yx} = 0$. Upper index M in the summation determines the flatness of the intensity profile of the generated beam in the far zone, covering all the intermediate cases between Gaussian ($M=1$) and square-pulse ($M \rightarrow \infty$) profiles. More precisely, a beam propagating at distance z from the source plane was shown to have correlation matrix elements as:

$$J_{\alpha\beta}(\boldsymbol{\rho}_1, \boldsymbol{\rho}_2, z) = \frac{\sqrt{I_\alpha^0} \sqrt{I_\beta^0} B_{\alpha\beta}}{C_0} \sum_{m=1}^M \frac{(-1)^{m-1}}{m} \binom{M}{m} \frac{1}{\Delta_{\alpha\beta}^2} \exp\left(-\frac{\boldsymbol{\rho}_1^2 + \boldsymbol{\rho}_2^2}{4\Delta_{\alpha\beta}^2\sigma^2}\right) \quad (8)$$

where expansion coefficients have the form

$$\Delta_{\alpha\beta}^2 = 1 + \frac{z^2}{4\sigma^4 k^2} + \left[\frac{4\sigma^2}{m\delta_{\alpha\beta}^2} \right] \quad (9)$$

$k = 2\pi/\lambda$ being the wave number, λ being the wavelength.

3. Experimental setup

A low power, 2 mW, HeNe vertically polarized laser source (A) was used to generate a Gaussian beam with a diameter of 0.5 mm (see Figures 1 and 2). A beam expander (B) was employed to expand the beam for filling the spatial light modulator window. The expanded beam was split with a 50/50 beam splitter (C) to generate vertically and horizontally polarized branches. In the horizontal branch, a half-wave plate (D) is inserted to rotate the beam generated by laser (A). The field is then reflected from the SLM (E) used to modulate the phase of horizontally polarized beam and it was aligned accordingly. A neutral density filter (F) is placed to adjust the power level for equalizing the power levels in both horizontal and vertical branches. To ensure stability of the degree of polarization, we used a linear polarizer (G). The vertical branch has SLM (E) (vertically oriented) neutral density filter (G) and the mirror (H) to redirect the beam for effective combination. When the beams in two branches are superimposed, a single partially polarized beam is formed from two polarized beams. Vertically and horizontally polarized beams are combined at a 50/50 Pellicle beam splitter (I), passing through a mechanical iris (J) to reduce diffraction effects. After passing through the iris, the beam passes through the turbulence emulator (L) and is captured by a polarimeter (M) sending the data to the computer (K).

The hot-air turbulence emulator configuration for this laboratory experiment (L in Figures 1 and 2) was approximately 15.2 cm in height, width, and depth. In characterizing the hot-air turbulence emulator, four thermocouple probes were used to measure the vertical and horizontal temperature differences of the beam propagation path and connected to a data logger that collected temperature readings every 1 s.

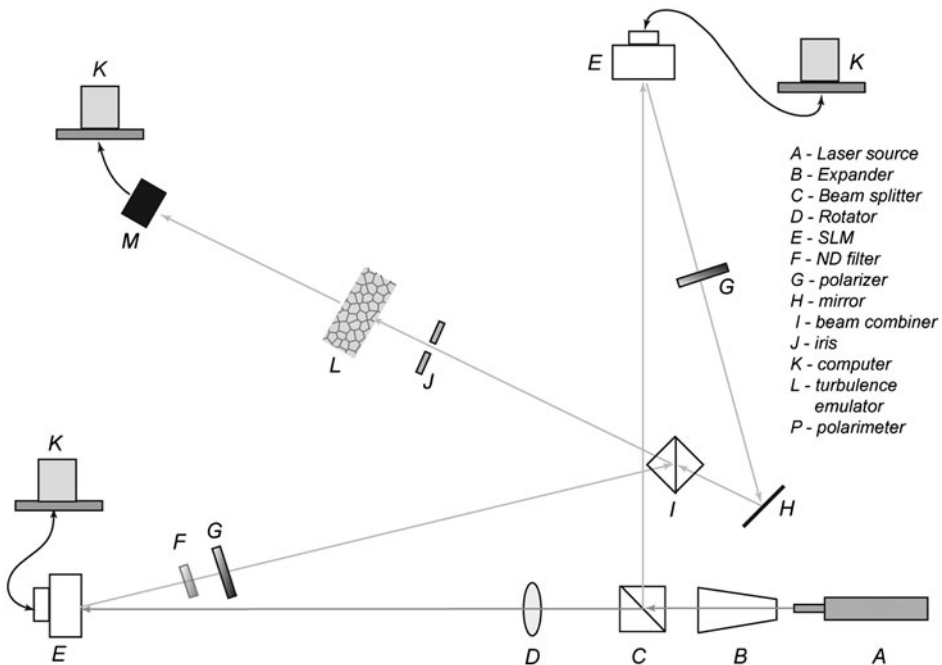


Figure 1. Experimental procedure for generating electromagnetic random beams.

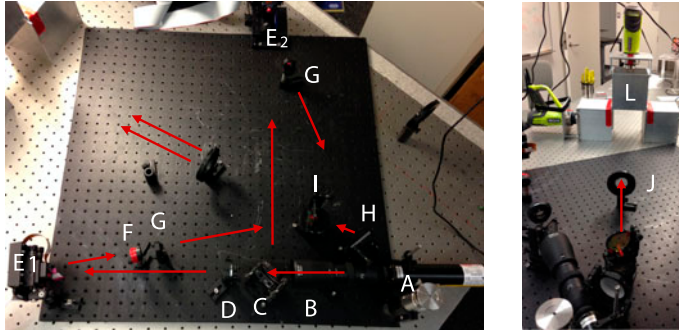


Figure 2. Photographs of (a) the system generating the beam; (b) the turbulence emulator.

The turbulence emulator was found to be approximately Kolmogorov along the beam propagation axis. This result was estimated through measurement of the temperature structure function, $D_T(r)$, as a function of thermocouple separation distance through the following equation,[26] known as the Kolmogorov–Obukhov similarity law [27]:

$$D_T(r) = \langle (T_1 - T_2)^2 \rangle = C_T^2 r^{2/3} \quad \text{for } l_0 \ll r \ll L_0 \quad (10)$$

where the separation distance between thermocouples, r , falls in the inertial subrange defined by the inner scale, l_0 , and outer scale, L_0 , of turbulence, and T_1 and T_2 are the thermocouple temperature readings in Kelvin.

Figure 3 shows a plot of $D_T(r)$ vs. $r^{2/3}$ for the hot-air turbulence emulator. The slope of the linear fit, over the range of approximately 2 mm – 5.2 cm gives an approximate value of the temperature structure constant, $C_T^2 = 14,012 \text{ K}^2/\text{m}^{-2/3}$ for the vertical direction, and $C_T^2 = 4872 \text{ K}^2/\text{m}^{-2/3}$ for the horizontal direction. Gamo and Majumdar [27] found a leveling of the temperature structure function after 7 cm for their experiment and explained this effect as where the separation distance between the temperature probes exceeded the outer scale of turbulence and where the temperature fluctuations between probes became uncorrelated. We did not see this leveling of the temperature structure function and therefore, we estimate the outer scale, L_0 , to be larger than 5.2 cm. The inner scale, l_0 , [26] is defined as the change over from $r^{2/3}$ to r^2 at small separation distances. Since we did not observe such a change we estimate the inner scale, l_0 , to be less than or in the order of 2 mm. This estimate for l_0 is in reasonable agreement with other measurements obtained using hot-air turbulence emulators,[28–31] where $l_0 \sim 5, 8, 3,$ and 6 mm respectively, and in general,[26] mentions that l_0 is typically $\sim 1 - 10$ mm near the ground.

Additionally, the refractive index structure parameter, C_n^2 , was approximated utilizing the following equation [26]:

$$C_n^2 = \left(77.8 \times 10^{-6} \frac{P}{T^2} \right) C_T^2, \quad (11)$$

where P is in millibars and T is in Kelvin.

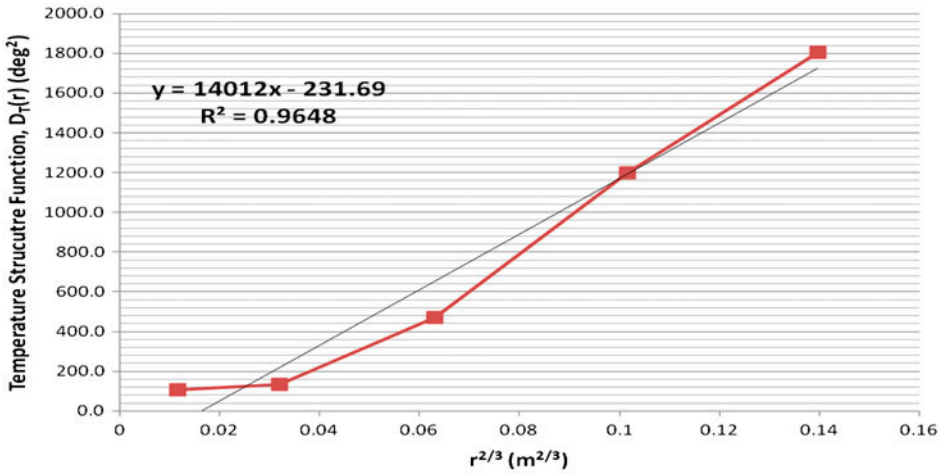


Figure 3. Plot of temperature structure function vs. thermocouple separation distance, $r^{2/3}$, for hot-air turbulence emulator in the vertical direction.

Where the temperature structure constant, C_T^2 was computed using Equation (10) at a specific thermocouple separation distance. C_T^2 was then used in Equation (11) to estimate C_n^2 for the section of hot-air turbulence emulator and then C_n^2 was averaged over the ~ 2 meter path length to give an approximate path-averaged value. A C_n^2 value of $10^{-18} \text{ m}^{-2/3}$ was used to estimate the turbulence strength for the open air propagation sections between source and receiver. The estimated values for the refractive index structure parameter were: $C_n^2 \sim 2.4 \times 10^{-10} \text{ m}^{-2/3}$ for the vertical and $C_n^2 \sim 8.9 \times 10^{-11} \text{ m}^{-2/3}$ for the horizontal direction.

Additionally, for comparison of laboratory to field results, the ratio of the source diameter, D_s to the spatial coherence radius, ρ_0 , or D_s/ρ_0 , is an important scaling parameter for turbulence emulation, and is discussed in a number of papers.[29,33] For our laboratory experimental setup, $D_s/\rho_0 \sim 2$, where ρ_0 was computed from,[26] and the Fresnel number, $N_f \sim 5$, computed from.[33] The Fresnel number is used to compare the relative level of near-to-far-field propagation of the beam. As a comparative example, these laboratory estimates would approximately scale to a field experiment with characteristics: transmitting aperture of 10 cm in diameter, wavelength of 632.8 nm, propagation distance of ~ 800 m, and atmospheric turbulence level of $C_n^2 \sim 1 \times 10^{-15} \text{ m}^{-2/3}$.

4. Results

Experiments consisted of several steps that verified conditions and number of repetitions to establish the reliability of the results. The first step is the adjustment of power for each polarization. Figure 4 shows the power readings for horizontally and vertically polarized beams, and their combination. The measured average light intensity at the receiver for the horizontally polarized beam was $0.49 \mu\text{W}$, for the vertically polarized beam $0.47 \mu\text{W}$, and for the combined power $0.95 \mu\text{W}$. The beams propagated in this experiment are multi-Gaussian beams (flat top) with correlation width of 0.021 mm. There were 40 ($M=40$) Gaussian beam contributions in the generation of each beam.

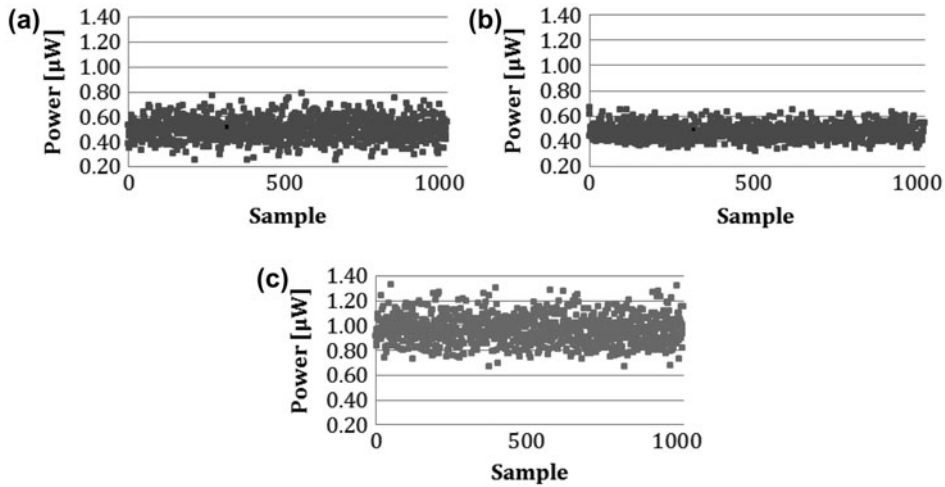


Figure 4. Measured power for (a) horizontally, (b) vertically polarized, and (c) combined vertically and horizontally polarized beams. Measured average powers are 0.49, 0.47, and 0.95 μW , respectively.

Screens with this statistics were cycled at the rate of 90.9 Hz to closer demonstrate theoretical assumptions. Since a single laser source was used in the experiment, we placed neutral density filters in each branch and adjusted the attenuation until we had matched powers for each polarization. Figure 4 clearly demonstrates a good match for each polarization and also shows the additive nature of the combined beam.

The next step in verifying the experimental conditions is adjustment of the azimuth angle for each beam. The polarizers were used to assure the polarization of 0° and 90° as it is indicated in Figure 5. Figure 5 also shows the instantaneous measurements of the degree of polarization in the combined beam. The same type of beams is propagated here, as described in discussion in Figure 4.

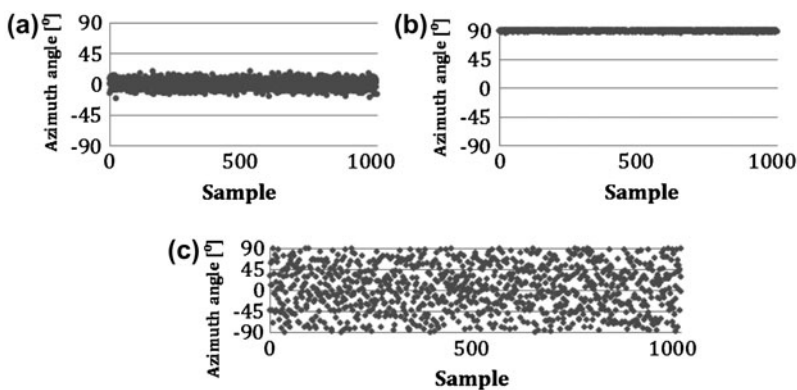


Figure 5. Azimuth angle for (a) horizontally polarized beam, (variance 48° , mean value -0.08°), (b) vertically polarized beam (variance 0.7° , mean value 88.9°), and (c) combined vertically and horizontally polarized beams (variance 2379° , mean value -3.17°).

Figure 6 shows the scintillation index for beams with multi-Gaussian correlations generated using cycling of the screens with prescribed statistics using an SLM (as given in Figure 4). Using Equation (4), the scintillation index was calculated for test 1 to be 0.01 and for test 2 to be 0.012, showing an excellent agreement and is a clear validation of Equation (4). This experiment has several contributions. Namely, the scintillation index for the combined beam went from 0.00001 in the case where there was no turbulence to 0.010 in the case when turbulence was introduced. The turbulence was not isotropic as it is clearly seen that the horizontally polarized beam experiences stronger variations in the intensity, and yet the scintillation index for the combined beam was reduced as prescribed theoretically.

Figure 7 shows the scintillation index measured over six runs for the case when the screen that created multi-Gaussian beams with correlation width of 0.021 mm was

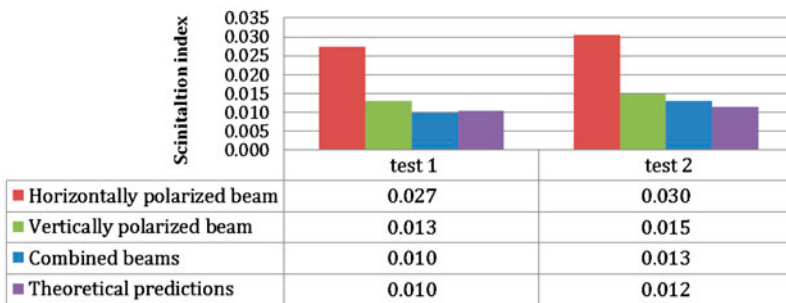


Figure 6. Scintillation index for multi-Gaussian beams with correlation width of 0.021 mm propagated through a laboratory-created turbulence. Screens with the prescribed statistics were cycling. Measured average degrees of polarization were 100% (horizontally polarized beam) 99.8% (vertically polarized beam), and 18.7% for the combined beams. Measured scintillation for the combined beam when no turbulence was induced was 0.00001 and the power was 0.95 μ W.

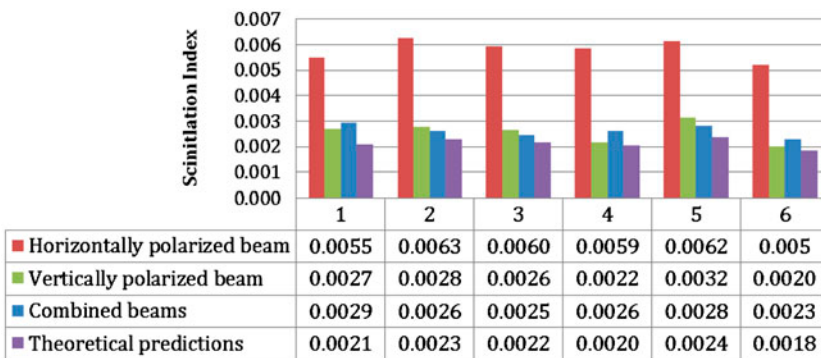


Figure 7. Scintillation index for multi-Gaussian beams with correlation width of 0.021 mm propagated through a laboratory-created turbulence. Screens with the prescribed statistics were stationary. Measured average powers were 0.48 μ W (horizontally polarized beam), 0.47 μ W (vertically polarized beam), and 0.94 μ W for the combined beams.

stationary. The turbulence conditions were the same as in Figure 4. Measured average powers were $0.48 \mu\text{W}$ (horizontally polarized beam), $0.47 \mu\text{W}$ (vertically polarized beam), and $0.94 \mu\text{W}$ for the combined beams. The main result from this set of experiments is that reduction in scintillation is significant and approaches the values suggested by the theory even though the beam was stationary. From Figure 7, the average measured scintillation index for the combined beams is 0.0026, and theoretical predictions using formula (4) is 0.0021 (for many realizations), showing good agreement.

5. Summary

The experimental demonstration of the recently theoretically predicted effect of scintillation reduction in a random electromagnetic optical wave propagating in a weakly turbulent medium has been reported. The optical beam of the electromagnetic multi-Gaussian Schell-model class has been realized with the help of the Mach–Zender interferometer which accepted a coherent laser beam and split it into two branches with orthogonal orientations. The two scalar beams were modulated in phase by two SLMs and finally superimposed. The resulting beam was passed through a turbulent air flow with the structure parameter C_n^2 that can be controlled by changing the input temperature. The obtained time series of the beam intensity and polarization properties were examined. Several experiments with modulation in (separately) vertical, horizontal polarization components, and their combinations have been compared with regards to the scintillation properties.

Our results clearly demonstrate that, in the case when two uncorrelated orthogonal polarization components are involved, the scintillation is reduced. The data showed good agreement with the previous theoretical predictions. Being the first experimental attempt to explore such polarization diversity, our study can prove very important for operation of optical systems in the presence of the atmospheric turbulence.

Acknowledgments

O. Korotkova acknowledges Stephen Guth for helpful discussions on theory and experimentation as well as strong technical support with instrumentation.

Funding

O. Korotkova's research is sponsored by US ONR (#N00189-14-T-0120) and US AFOSR (#FA9550-12-1-0449). Svetlana Avramov-Zamurovic, Reza Malek-Madani, and Charles Nelson are sponsored by ONR (N0001413WX20152).

References

- [1] Carl Leader J. Intensity fluctuations resulting from partially coherent light propagating through atmospheric turbulence. *J. Opt. Soc. Am.* 1979;69:73–84.
- [2] Banakh VA, Buldakov VM. Effect of the initial degree of spatial coherence of a light beam on intensity fluctuations in a turbulent atmosphere. *Opt. Spectrosc.* 1983;55:707–712.
- [3] Ricklin JC, Davidson FM. Atmospheric turbulence effects on a partially coherent Gaussian beam: implications for free-space laser communication. *J. Opt. Soc. Am. A.* 2002;19:1794–1802.

- [4] Ricklin JC, Davidson FM. Atmospheric optical communication with a Gaussian Schell beam. *J. Opt. Soc. Am. A.* 2003;20:856–866.
- [5] Korotkova O, Andrews LC, Phillips RL. Model for a partially coherent Gaussian beam in atmospheric turbulence with application in lasercom. *Opt. Eng.* 2004;43:330–341.
- [6] Churnside JH. Aperture averaging of optical scintillations in the turbulent atmosphere. *Appl. Opt.* 1991;30:1982–1994.
- [7] Rosenberg S, Teich MC. Photocounting array receivers for optical communication through the lognormal atmospheric channel 2: optimum and suboptimum receiver performance for binary signaling. *Appl. Opt.* 1973;12:2625–2634.
- [8] Lee EJ, Chan VWS. Part 1: optical communication over the clear turbulent atmospheric channel using diversity. *IEEE J. Select. Areas Commun.* 2004;22:1896–1906.
- [9] Berman GP, Bishop AR, Chernobrod BM, Nguyen DC, Gorshkov VN. Suppression of intensity fluctuations in free space high-speed optical communication based on spectral encoding of a partially coherent beam. *Opt. Commun.* 2007;280:264–270.
- [10] Berman GP, Chumak AA. Influence of phase-diffuser dynamics on scintillations of laser radiation in Earth's atmosphere: long-distance propagation. *Phys. Rev. A.* 2009;79:063848–063854.
- [11] Korotkova O. Scintillation index of a stochastic electromagnetic beam propagating in random media. *Opt. Commun.* 2008;281:2342–2348.
- [12] Gu Y, Korotkova O, Gbur G. Scintillation of nonuniformly polarized beams in atmospheric turbulence. *Opt. Lett.* 2009;34:2261–2263.
- [13] Xiao X, Voelz D. Wave optics simulation of partially coherent and partially polarized beam propagation in turbulence. *Proc. SPIE 7464, Free-Space Laser Communications IX, 74640T*; 2009 Aug 21; San Diego, CA.
- [14] Piquero G, Gori F, Romanini P, Santarsiero M, Borghi R, Mondello A. Synthesis of partially polarized Gaussian Schell-model sources. *Opt. Commun.* 2002;208:9–16.
- [15] Shirai T, Korotkova O, Wolf E. A method of generating electromagnetic Gaussian Schell-model beams. *J. Opt. A: Pure Appl. Opt.* 2005;7:232–237.
- [16] Ostrovsky AS, Rodríguez-Zurita G, Meneses-Fabián C, Olvera-Santamaría MÁ, Rickenstorff-Parrao C. Experimental generating the partially coherent and partially polarized electromagnetic source. *Opt. Express.* 2010;18:12864–12871.
- [17] Chen Y, Wang F, Liu L, Zhao C, Cai Y, Korotkova O. Generation and propagation of a partially coherent vector beam with special correlation functions. *Phys. Rev. A.* 2014;89: 013801.
- [18] Avramov-Zamurovic S, Nelson C, Korotkova O, Malek-Madani R. The dependence of the intensity PDF of a random beam propagating in the maritime atmosphere on source coherence. *Waves in Complex and Random Media.* 2014;24:69–82.
- [19] Sahin S, Korotkova O. Light sources generating far fields with tunable flat profiles. *Opt. Lett.* 2012;37:2970–2972.
- [20] Korotkova O, Sahin S, Shchepakina E. Multi-Gaussian Schell-model beams. *J. Opt. Soc. Am. A.* 2012;29:2159–2164.
- [21] Mei Z, Korotkova O, Shchepakina E. Electromagnetic multi-Gaussian Schell-model beams. *J. Opt.* 2013;15:025705.
- [22] Nelson C, Avramov-Zamurovic S, Malek-Madani R, Korotkova O, Sova R, Davidson F. Measurements of partially spatially coherent laser beam intensity fluctuations propagating through a hot-air turbulence emulator and comparison with both terrestrial and maritime environments. In: Hemmati H, Boroson DM, editors. *Proceedings of SPIE 8610, Free-Space Laser Communication and Atmospheric Propagation XXV, 86100T*. San Francisco (CA): SPIE; 2013.
- [23] Wang F, Liu X, Liu L, Yuan Y, Cai Y. Experimental study of the scintillation index of a radially polarized beam with controllable spatial coherence. *Appl. Phys. Lett.* 2013;103:091102.

- [24] Gori F. Matrix treatment for partially polarized, partially coherent beams. *Opt. Lett.* 1998;23:241–243.
- [25] Wolf E. Unified theory of coherence and polarization of random electromagnetic beams. *Phys. Lett. A.* 2003;312:263–267.
- [26] Andrews LC, Phillips RL. *Laser beam propagation through random media.* 2nd ed. Bellingham, WA: SPIE Press; 2005.
- [27] Gamo H, Majumdar A. Atmospheric turbulence chamber for optical transmission experiment: characterization by thermal method. *Appl. Opt.* 1978;17:3755–3762.
- [28] Gamo H, Majumdar AK. Atmospheric turbulence chamber for optical transmission experiment: characterization by thermal method. *Appl. Opt.* 1978;17:3755–3762.
- [29] Keskin O, Jolissaint L, Bradley C. Hot-air optical turbulence generator for the testing of adaptive optics systems: principles and characterization. *Appl. Opt.* 2006;45:4888–4897.
- [30] Majumdar AK, Gamo H. Statistical measurements of irradiance fluctuations of a multipass laser beam propagated through laboratory-simulated atmospheric turbulence. *Appl. Opt.* 1982;21:2229–2235.
- [31] Masciadri E, Vermin J. Optical technique for inner-scale measurement: possible astronomical applications. *Appl. Opt.* 1997;36:1320–1327.
- [32] Phillips JD. *Atmospheric turbulence simulation using liquid crystal spatial light modulators* [masters thesis], Ohio: Wright-Patterson Air Force Base; 2005.
- [33] Goodman JW. *Introduction to Fourier optics.* 2nd ed. McGraw-Hill Higher Education; 1996.